Electronic Supplementary Information

Simple and effective fabrication of Sb_2Te_3 films embedded with Ag_2Te nanoprecipitates for enhanced thermoelectric performance

Jiwon Kim,[a] Kyu Hyoung Lee,[b] Sung-Dae Kim,[c] Jae-Hong Lim,[a*] and Nosang V. Myung[d*]

[a]Electrochemistry Research Group, Materials Processing Division, Korea Institute of Materials Science, Changwon-si, Gyeongnam 51508, Republic of Korea

[b]Department of Nano Applied Engineering, Kangwon National University, Chuncheon-si, Kangwon 24341, Republic of Korea

[c]Materials Modeling & Characterization Department, Korea Institute of Materials Science, Changwon-si, Gyeongnam 51508, Republic of Korea

[d]Department of Chemical and Environmental Engineering and Winston Chung Global Energy Center, University of California-Riverside, Riverside, California 92521, USA

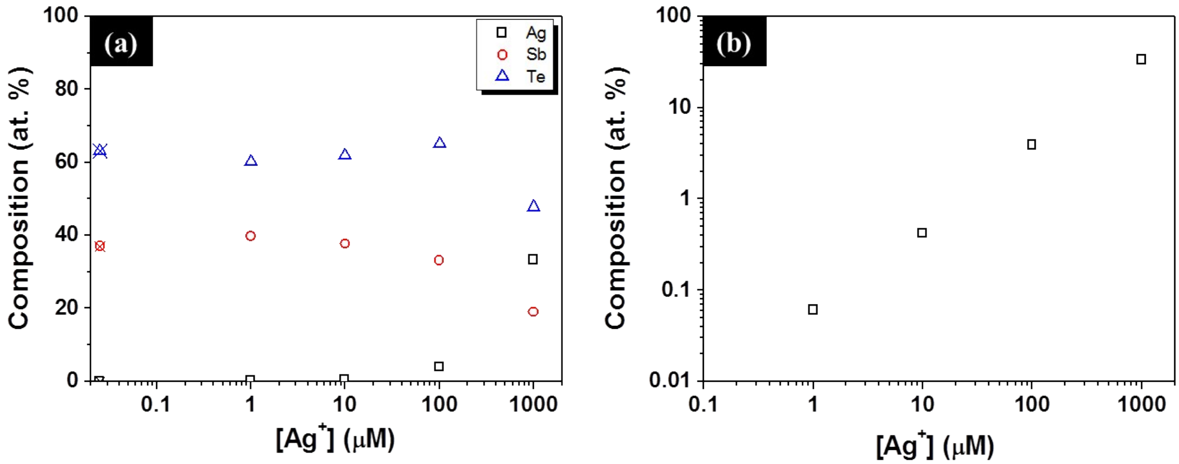

Figure S1. (a) Compositions of the $Ag_xSb_yTe_z$ films as a function of Ag^+ concentration. The electrolyte employed consisted of 2.4 mM $HTeO_2^+$, 3.6 mM $[Sb(C_4H_2O_6)_2]^{2-}$, 33 mM $C_4H_6O_6$, and 1 M HNO_3. The Ag^+ concentration was varied from 0 to 1000 μM. The triangles, circles, and squares denote Te, Sb, and Ag, respectively. The applied potential was fixed at −0.1 V (vs. SCE). (b) For clarity, the Ag compositions are also plotted on a logarithmic scale.

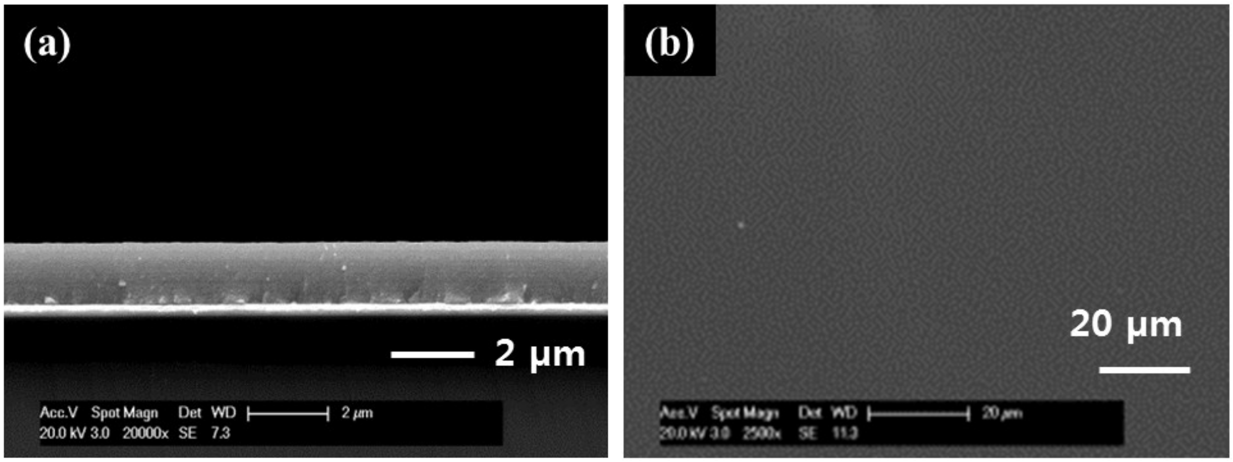

Figure S2. SEM images of the $Ag_{3.9}Sb_{33.6}Te_{62.5}$ film. (a) and (b) show a cross-section and the surface morphology of the film, respectively.

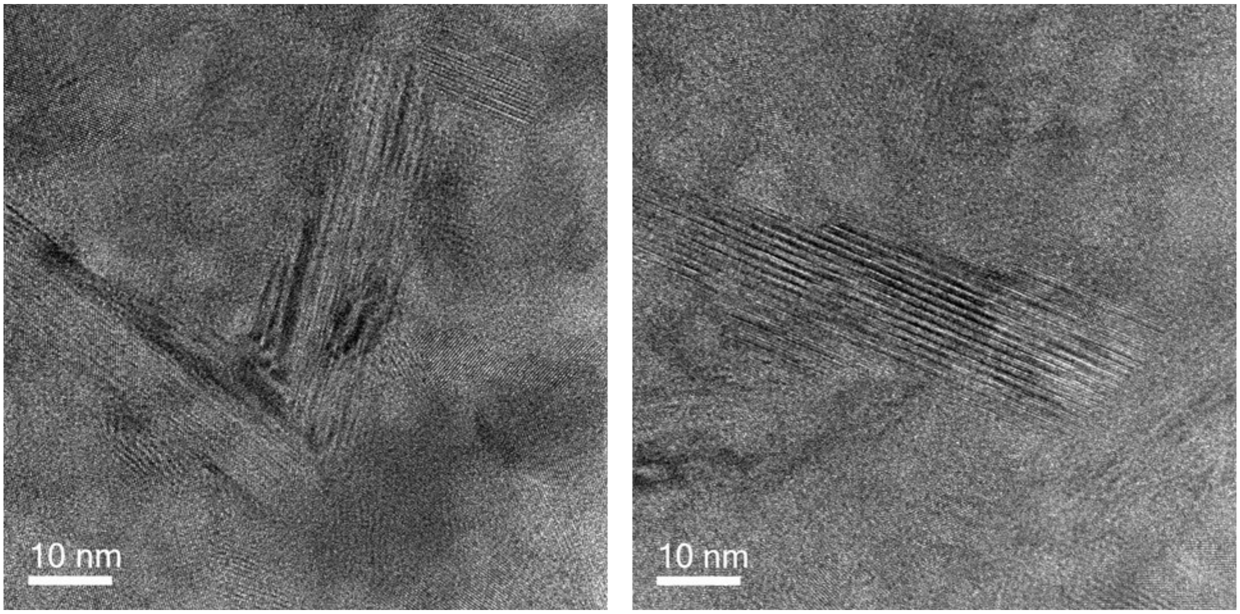

Figure S3. TEM images showing the precipitated Ag_2Te nanodots in the Sb_2Te_3 matrix.

Table S1. Electrical properties of the $Ag_{3.9}Sb_{33.6}Te_{62.5}$ films as a function of annealing temperature

annealing temperature	**conductivity**	**carrier conc.**	**mobility**
(°C)	**($S \cdot cm^{-1}$)**	**(cm^{-3})**	**($cm^{2} \cdot V^{-1} \cdot s^{-1}$)**
as-prepared	4.32×10^{-2}	1.81×10^{17}	0.88
40	5.23×10^{-2}	2.91×10^{17}	0.66
50	4.97×10^{-2}	2.39×10^{17}	0.76
60	5.12×10^{-1}	2.26×10^{18}	0.83
70	5.52	2.34×10^{19}	0.87
80	2.83×10^{1}	1.86×10^{19}	5.58
90	8.20×10^{2}	1.99×10^{20}	15.11
100	1.82×10^{3}	1.86×10^{20}	35.97

As shown in Table S1, the carrier concentrations of the film samples varied from 10^{17} to 10^{20} cm^{-3} as the crystallinity increased. In addition, we found that the mobility increased with increasing annealing temperature, which is consistent with the enhancement of crystallinity observed for the various film samples.